Virtual Electrode–Induced Reexcitation
A Mechanism of Defibrillation

Yuanna Cheng, Kent A. Mowrey, David R. Van Wagoner, Patrick J. Tchou, Igor R. Efimov

Abstract—Mechanisms of defibrillation remain poorly understood. Defibrillation success depends on the elimination of fibrillation without shock-induced arrhythmogenesis. We optically mapped selected epicardial regions of rabbit hearts (n=20) during shocks applied with the use of implantable defibrillator electrodes during the refractory period. Monophasic shocks resulted in virtual electrode polarization (VEP). Positive values of VEP resulted in a prolongation of the action potential duration, whereas negative polarization shortened the action potential duration, resulting in partial or complete recovery of the excitability. After a shock, new propagated wavefronts emerged at the boundary between the 2 regions and reexcited negatively polarized regions. Conduction velocity and maximum action potential upstroke rate of rise dV/dt_{max} of shock-induced activation depended on the transmembrane potential at the end of the shock. Linear regression analysis showed that dV/dt_{max} of postshock activation reached 50% of that of normal action potential at a V_m value of -56.7 ± 0.6 mV postshock voltage (n=9257). Less negative potentials resulted in slow conduction and blocks, whereas more negative potentials resulted in faster conduction. Although wavebreaks were produced in either condition, they degenerated into arrhythmias only when conduction was slow. Shock-induced VEP is essential in extinguishing fibrillation but can reinduce arrhythmias by producing excitable gaps. Reexcitation of these gaps through progressive increase in shock strength may provide the basis for the lower and upper limits of vulnerability. The former may correspond to the origination of slow wavefronts of reexcitation and phase singularities. The latter corresponds to fast conduction during which wavebreaks no longer produce sustained arrhythmias. **(*Circ Res*. 1999;85:1056-1066.)**

Key Words: conduction ■ fibrillation ■ polarization ■ mapping ■ defibrillation

The goal of defibrillation shocks is to resynchronize electrical activity to restore contractile function. Although the exact mechanisms of defibrillation are still poorly understood, it is clear that 2 main processes determine the success of a defibrillation shock. First, the defibrillation shock must extinguish irregular electrical activity. Second, the shock itself must not produce a new arrhythmia. Several theories have been proposed in an attempt to explain the mechanisms of defibrillation, but recent studies using high-resolution imaging of electrical activity during defibrillation shocks[1] provide evidence of several inconsistencies in these theories.

One theory[2,3] proposes the commonly accepted mechanism of extinguishing fibrillatory activity. According to this theory, resynchronization occurs through shock-induced prolongation of refractory periods (RPs) or action potential (AP) durations (APDs). However, our recent data suggest[1] that due to the virtual electrode (VE) effect,[4] APDs and RPs will be prolonged in some areas of myocardium while they shortened in other areas. These are areas of positive and negative polarization, respectively. Therefore, VEs may create a dispersion of repolarization.

There is no commonly accepted theory regarding the mechanisms of postshock arrhythmias that underlie defibrillation failure. Two alternative ideas are often considered: (1) persistent fibrillatory activity due to unextinguished wavelets or due to focal activity and (2) shock-induced new wavefronts and reentry. The first appears to be commonly accepted,[5] whereas the second remains debatable.[6] The upper limit of vulnerability theory, and specifically its critical point hypothesis,[7] suggests that new reentrant wavefronts develop when a low-voltage gradient occurs in excitable gaps in the fibrillation. However, others have suggested[8] that new wavefronts can be induced in fully refractory tissue. The mechanisms of this excitation remain unclear.

As suggested in our previous study,[1] the VE effect may be responsible for at least 2 apparently proarrhythmic effects: (1) simultaneous prolongation and shortening of APDs may create significant dispersion of repolarization, and (2) new shock-induced wavefronts can interact with this APD dispersion and develop block of conduction that results in wavebreaks and reentrant arrhythmias. A wavebreak is a critical point between propagating wavefront and the line of block.

The role of VEs in successful monophasic defibrillation is controversial. Any monophasic shock will produce VEs. Therefore, why do some VEs result in phase singularity and arrhythmia and others do not? We hypothesized that the

Received July 9, 1999; accepted September 21, 1999.

From the Department of Cardiology, Cleveland Clinic Foundation, Cleveland, Ohio.

Correspondence to Igor R. Efimov, PhD, Department of Cardiology, Desk FF1, Cleveland Clinic Foundation, 9500 Euclid Ave, Cleveland, OH 44195. E-mail efimov@ieee.org

Circulation Research **is available at http://www.circresaha.org**

shortening of APD produced by the negative polarization is the key. Shortening of APD by an intracellular stimulus applied during the RP is a well known effect that has been demonstrated in isolated cells, fibers, and tissue strips.[9–12] This effect has been termed "deexcitation," "immediate repolarization," "forced repolarization," "regenerative repolarization," and "all-or-nothing repolarization." It is also referred to as "hyperpolarization" when the transmembrane voltage is more negative than the resting potential.

Until our recent study,[1] the effect of deexcitation had not been observed in the intact heart during extracellular stimulation. We hypothesized that this effect not only is present during defibrillation shocks but also may play a major role in the success and failure of defibrillation therapy. We quantitatively investigated the genesis and conduction of shock-induced wavefronts and wavebreaks and their relation to deexcitation. Our data provide mechanistic insights into defibrillation, as well as the lower and upper limits of vulnerability.

Materials and Methods

Detailed protocols have been previously published.[1,13] Langendorff-perfused rabbit hearts (n=20) were paced at the apex at a 300-ms cycle length with 2-ms pulses. Hearts were stained with 20-μmol/L di-4-ANEPPS (Molecular Probes) during 5 to 10 minutes. Temperature and pH were maintained at 36±0.5°C and 7.35±0.05, respectively. 2,3-Butanedione monoxime (BDM; 15 mmol/L; Fisher Chemical) was added. Monophasic shocks (150 μF, 8 ms, ±20 to 300 V) were delivered 100 ms after the average activation time with the use of a defibrillator (HVS-02; Ventritex) between the 2 coil electrodes.[13]

Fluorescence was excited at 520±45 nm and collected above 610 nm with the use of a photodiode array (C4675; Hamamatsu). Spatial and temporal resolution of optical recordings was 375 to 970 μm and 528 μs, respectively. The signal-to-noise ratio (SNR_{RMS}) was 250±80. Transmembrane voltage was calculated from fluorescent recordings with the use of a pseudo-mV calibration.[14] We assumed that the normal AP has a 100-mV amplitude and a −85-mV resting potential.

Optical recordings represent the average electrical activity of a large number of cells. The observed dF/dt during optical AP upstroke depends on the conduction velocity, spatial resolution, and optical depth of field.[15] Therefore, the absolute rate of rise during cellular AP upstroke cannot be measured from optical recordings. We estimated the rate of rise during shock-induced responses (postshock dF/dt) with respect to that of the normal AP upstroke dF/dt by calculating their ratio. Here, we refer to this ratio as the upstroke rate of rise dV/dt_{max} of postshock activation.

To correlate the rate of postshock excitation with the degree of deexcitation produced by negative polarization, we measured the dV/dt_{max} of upstrokes of optical postshock responses. We hypothesized that this rate would depend on the excitability of deexcited cells. Excitability is determined by 2 factors: the degree of deexcitation produced by negative polarization, and the time lapsed after the shock withdrawal. The latter component does not depend on shock-induced VE polarization (VEP) and thus was considered to be a contamination of the studied phenomenon. Therefore, we designed inclusion criteria that would automatically remove this contamination. We included in our analysis only the records of postshock excitation that were excited between 5 and 30 ms after the shock withdrawal. Furthermore, the rate of excitation depends on the driving force, which is especially important at the boundary between areas of positive and negative polarization. Although the process at the boundary is an important phenomenon in the genesis of wavefront via break excitation, this effect would also contaminate the studied correlation between the deexcitation and the rate of postshock excitation that occur at a distance from the boundary. Therefore, we also excluded this effect by considering only the sites that were deexcited by >-20 mV from the preshock transmembrane voltage. Such criterion effectively excluded areas at the boundary between the oppositely polarized regions.

To automatically process the large amounts of data, a program was developed with the use of C++. This program used a 5-point boxcar filter and automatically calculated postshock transmembrane voltage, dV/dt_{max}, and APD as described earlier. No manual correction was required except in APD measurements. Data are expressed as mean±SD.

Results

VEs Simultaneously Prolong and Shorten APD

Conventional electrode and optical recordings provided evidence that a strong electric shock prolongs APD and RP.[2,16] This effect became a key element of the theory of defibrillation; however, with this theory, we could not explain how shocks of either polarity could both prolong APDs. We investigated this apparent paradox.

The first striking finding was the observation that the APD may be both prolonged and shortened at the same time in different areas of the epicardium due to the VE effect. Figure 1A shows a postshock map of transmembrane voltage at the end of −100-V shock applied during the RP of a normal AP. Positive polarization was produced next to the right ventricular (RV) electrode (not shown) in the left half of the field of view. Negative polarization was observed in the adjacent left ventricular (LV) area (right half of the field of view). Figure 1B shows a map of postshock activation. The sites of the origin of the wavefront of postshock activation are shown in white and located at both sides of the positively polarized areas (compare with panel A). Activation spread along an arrow, forming reentry. Figure 1C shows 15 raw traces recorded sequentially along this arrow. As seen from these traces, shortening and prolongation of APD was produced by negative and positive polarization, respectively. Figure 1D further illustrates these observations in all 256 unfiltered traces recorded during this shock-induced arrhythmia.

We investigated the simultaneous prolongation and shortening of APD in 5 experiments in which the shock electrode was placed in the LV. This electrode position was chosen because it was less likely to result in an arrhythmia compared with an RV shock. As shown in Figure 1C and 1D, the onset of an arrhythmia would make it impossible to measure the APD of the postshock response. The top panels of Figure 2 show maps of transmembrane voltage at the end of an anodal monophasic (+200 V) shock (left) and the APD_{90} of normal (middle) and a shock-altered (right) responses. These data were recorded from a 15.5×15.5-mm area of the LV epicardium. The bottom panel of Figure 2 shows representative traces recorded from the areas selected with black boxes in the top panels. Two superimposed maps of optical recordings are shown: APs recorded during the last basic beat and during a shock at the boundary between the positively (red traces) and negatively (blue traces) polarized areas. Notice that APDs were shortened in the area of negative polarization. In contrast, APDs were prolonged in the area of positive polarization. This resulted in a significant dispersion of repolarization.

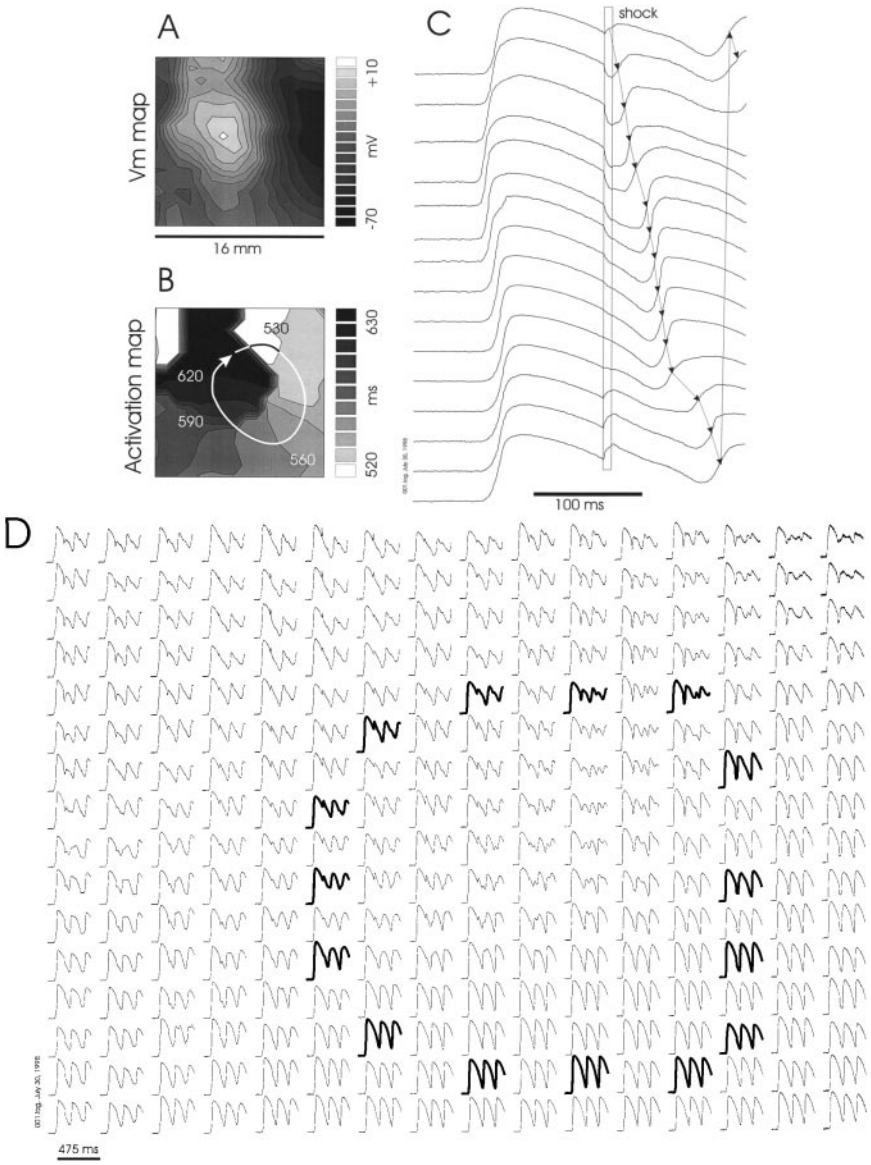

Figure 1. VE-induced arrhythmia. A, VEP developed at end of monophasic cathodal shock (−100 V, 8 ms). B, Post-shock activation resulting from VEP. Shock lasted from 512 to 520 ms. C, Raw optical recordings collected around VE-induced phase singularity area. Recording sites were sequentially selected along circular arrow in panel B. D, 256 optical recordings during 2 initial periods of arrhythmia resulted from VE-induced phase singularity. Bold traces are shown in C.

In contrast, Figure 3 shows responses that appear as APD prolongation in all areas. These data were recorded when the shock strength was increased to +300 V. As evident from the representative traces shown in the bottom panel and the maps of APDs in the top panels, there was little difference in the areas of positive polarization (red traces) but a dramatic change in the areas of negative polarization (blue traces) compared with Figure 2. Repolarization times in the positively polarized areas were progressively prolonged with increases in shock strength from +100 (not shown) to +300 V. On the contrary, in the area of negative polarization, repolarization times were first shortened and then prolonged with shocks ranging from +100 to +300 V. Is this bimodal response caused by shock-induced prolongation of APD or by a new response? And if it is caused by a new response, what is the origin of this response?

Figure 4 illustrates the transmembrane voltage distribution at the end of shocks (+100, +200, and +300 V) along a horizontal line shown in the top left panels of Figures 2 and 3. The voltage gradient between positively and negatively polarized areas progressively increased with increasing in shock intensity. Areas of negative polarization reached −23.8, −41.9, and −52.8 mV, for +100-, +200-, and +300-V shocks, respectively. As evident from Figures 2 and 3, only the +300-V shock produced an extension of recovery time in the negatively polarized area. The Table summarizes the average extension of APD (ΔAPD_{90}) that resulted from shocks of different amplitude and either polarity (7950 analyzed recordings, 5 hearts). Asterisks in the Table indicate data that contained both shortening and prolongation of APD in different channels; daggers indicate that data were measured when no shortening was observed. Averaging of ΔAPD_{90} was done across the entire field of view, including both positive (prolongation) and negative (shortening) polarizations.

Modulation of Negative Polarization and Rate of Rise of Postshock Excitation by Shock Intensity

Analysis of the transition from APD shortening to APD prolongation is complicated due to the spatial heterogeneity

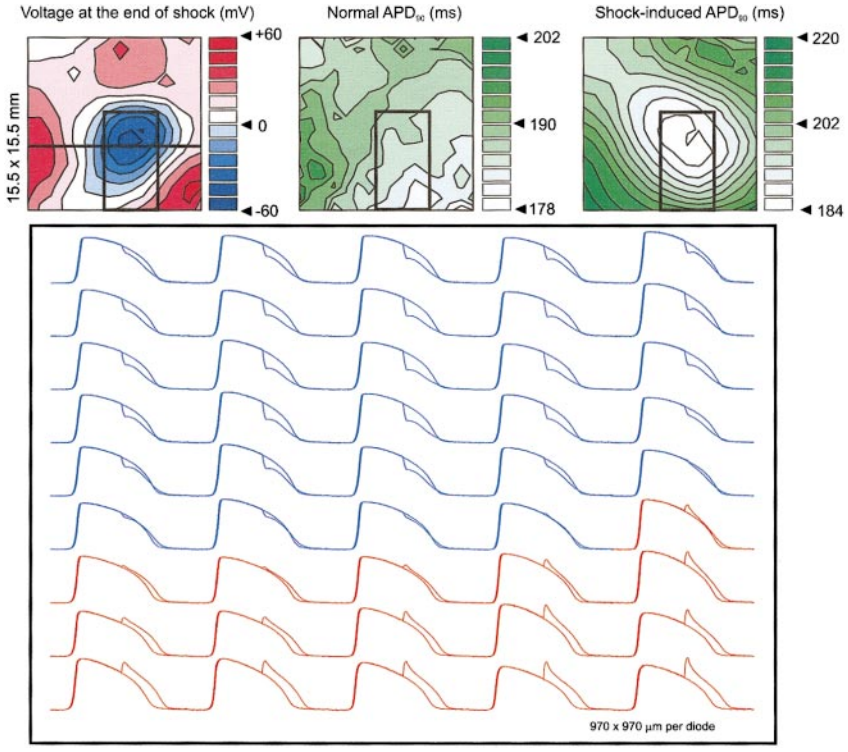

Figure 2. Negative and positive polarizations induced by a monophasic shock (+200 V, 8 ms) cause AP shortening and prolongation, respectively. Electrical activity was recorded from a 15.5×15.5-mm area of LV epicardium. Each of 256 traces was recorded from 970×970 μm. Left top, LV epicardial transmembrane voltage distribution at end of shock applied endocardially in LV. Horizontal line shows position of recording sites summarized in Figure 4. Middle top, Map of APDs (APD_{90}) during a normal basic beat. Right top, Map of APD_{90} of shock-induced responses. Bottom, Superimposed representative traces recorded during last basic beat and shock-induced response. These traces were recorded from an area selected with black box in top panels. Data from areas with prolonged APDs are shown in red, and those with shortened APDs are shown in blue.

of the polarization and due to the rapid postshock excitation that usually follows the shock withdrawal (Figure 5). Therefore, we chose to evaluate the degree of shock-induced deexcitation and the recovery of excitability based on the rate of rise of postshock activation. Figure 5 summarizes the results of 1 experiment. Figure 5A shows a typical VEP pattern produced by a cathodal shock (−100 V). Figure 5B shows 7 superimposed optical traces recorded from the same site during shocks with different amplitudes (−60 to −260 V). As seen from the red trace in this figure, the weakest shock (−60 V) resulted in deexcitation and shortening of APD. An increase in shock intensity to −80 V (green trace) resulted in stronger negative polarization and a slowly rising postshock response, which was absent after the −60-V shock.

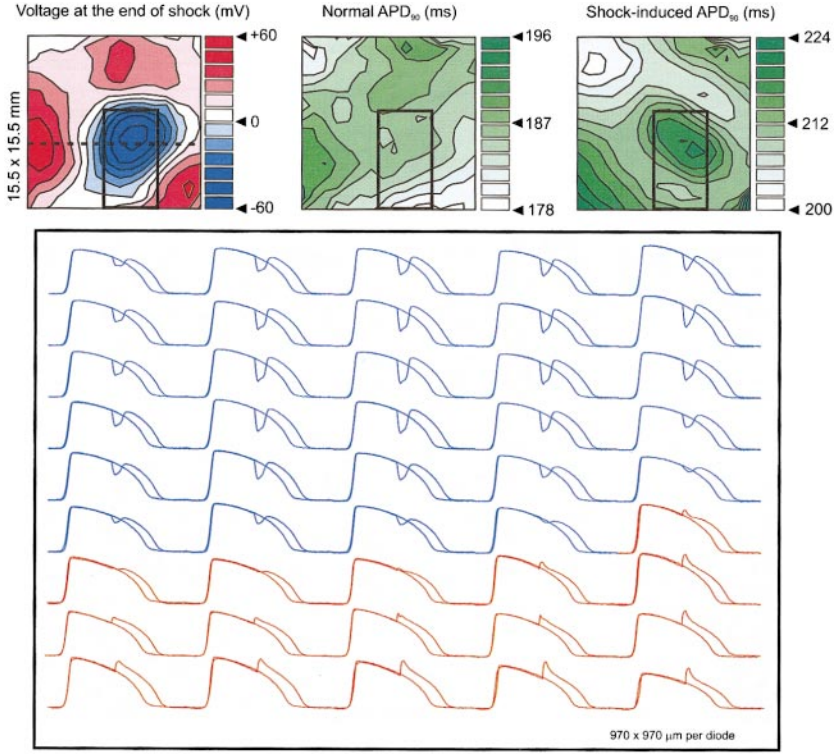

Figure 3. Negative and positive polarizations induced by a monophasic shock (+300 V, 8 ms) recorded from same area as in Figure 2. Left top, LV epicardial transmembrane voltage distribution at end of shock applied endocardially. Horizontal line, Position of recording sites summarized in Figure 4. Middle top, Map APD_{90} during a normal basic beat. Right top, Map of APD_{90} during shock-induced responses. Bottom, Superimposed representative traces recorded during last basic beat and shock-induced response. These traces were recorded from an area shown with black box in top panels. Data from an area with prolonged APDs is shown in red. Data from area of reexcitation is shown in blue (see details in text).

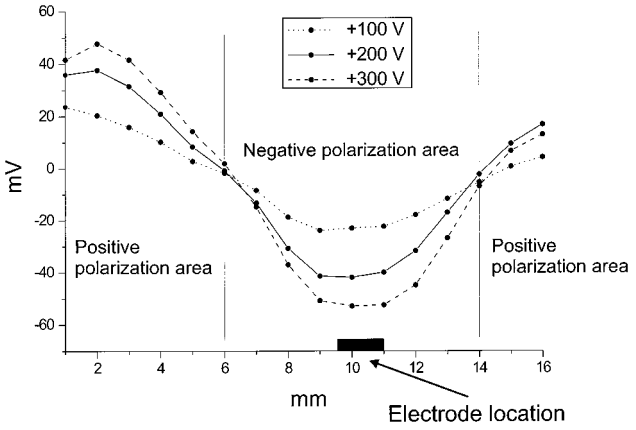

Figure 4. Transmembrane voltage gradient between areas of positive and negative polarizations. Epicardial transmembrane voltage distributions at end of 8-ms anodal monophasic shocks (+100, +200, +300 V) are shown. Data represent a 1-dimensional slice from 2-dimensional maps shown in Figures 2 and 3 for +200- and +300-V shock, respectively. See horizontal lines in top left panels of these figures for locations. The 100-V 2-dimensional map was not shown previously. Electrode endocardial location is shown with black box.

Further increases in shock intensity resulted in stronger negative polarizations and faster postshock responses. Figure 5C summarizes the data from all 7 shocks. This figure includes data from a total of 656 recording sites that were negatively polarized by the shock to >-20 mV relative to preshock value and that were activated between 5 and 30 ms after the shock withdrawal. There is a clear correlation between postshock transmembrane voltage and the rate of rise of postshock upstroke.

A linear regression analysis was used as the simplest possible approximation to quantitatively analyze this distribution. It resulted in the following equation: $dV/dt_{relative}=A+B*V_m$, where A is -0.833 ± 0.047 and B is -0.024 ± 0.001 mV^{-1}. $dV/dt_{relative}$ refers to the ratio between the postshock dF/dt_{max} and that of the normal AP. $dV/dt_{relative}$ reached 50% at a V_m value of -55.5 ± 2.0 mV in this case. Figure 6 shows 8 additional individual experiments and a summary for 9 hearts. Linear regression analysis conducted on data from the 9 hearts with a total of 9257 recordings showed that dV/dt_{max} of reexcitation reached 50% of that of normal AP at a V_m value of -56.7 ± 0.6 mV. The remaining 6 experiments were qualitatively analyzed, and similar phenomena were observed. Thus, these observations were reproduced in all 15 hearts studied.

Shock-Induced Reexcitation and Propagated Activation Wavefronts

As follows, recovered regions may be subsequently excited and support an active, propagated response. Figure 7 demonstrates 1 such example. The top panel shows 8 optical recordings from a line of photodiodes identified in the diagram as 1 to 8. As evident from the activation map (bottom), recording sites were chosen along the conduction velocity vector (black arrow). All of these sites were negatively polarized at the end of a -100-V monophasic shock. As seen in the top panel of Figure 7, all 8 recording sites were

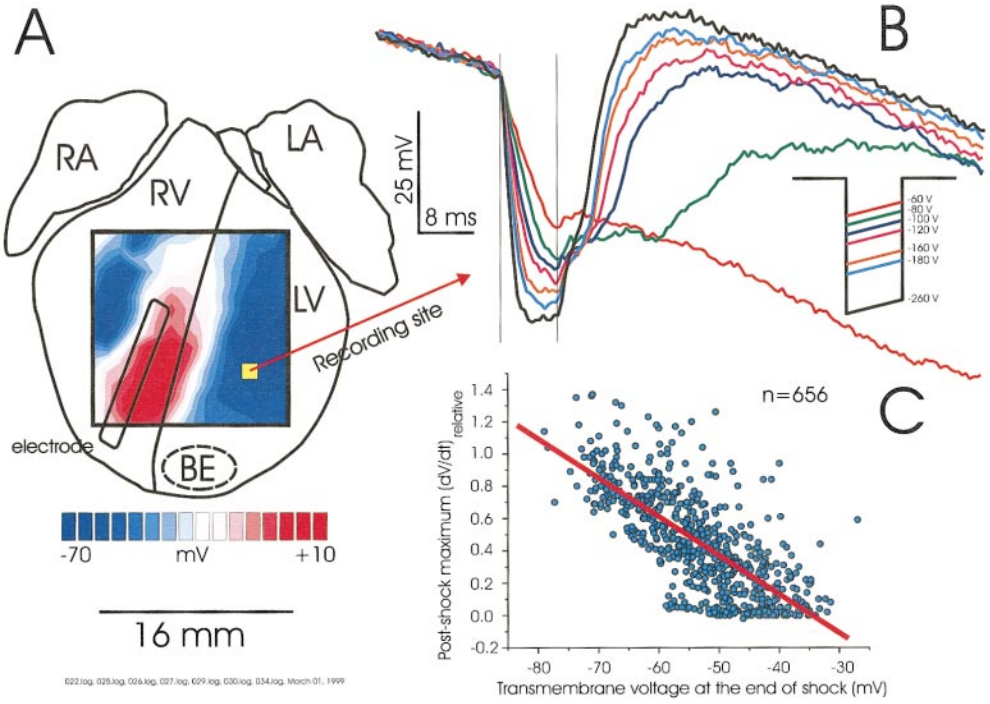

Figure 5. Cellular polarization and rate of postshock excitation depend on shock intensity. A, VE polarization at end of cathodal monophasic ICD shock is shown. RA indicates right atrium; LA, left atrium; and BE, bipolar electrode. B, Seven superimposed optical traces representing responses to 7 different monophasic shock intensities. Color of responses corresponds to color of shock waveforms shown in inset. Two vertical lines show onset and end of shock. All recordings were taken from a single site shown in panel A. C, Summary of rate of rise of postshock excitation versus transmembrane voltage at end of shock is shown. Data represent 656 recordings collected during 7 shocks illustrated in panel B. Only negatively polarized recordings areas activated within time frame of 5 to 30 ms after shock withdrawal were included (see Materials and Methods for details).

Average APD Extension (ΔAPD_{90}) Produced by LV Shocks

Experiment	±100 V	±200 V	±300 V
1	7.0±5.6*	11.2±11.8*	25.5±7.8†
2	36.2±12.4†	52.3±8.2†	57.3±12.6†
3	2.1±11.1*	28.7±6.5†	37.3±6.3†
4	37.9±13.7†	46.6±7.8†	49.9±8.0†
5	7.1±5.3*	19.6±4.2†	27.3±4.5†

*Data that contained both shortening and prolongation of APD in different channels.

†Measured when no shortening was observed.

sequentially reexcited. Excitation started from a site near the shock electrode and then spread away from the electrode. The sequence of reexcitation cannot be explained by the passive discharge of the membrane due to its propagative nature. A purely electrotonic response also fails to explain this sequential depolarization, because distant recordings sites are located more than several space constants away. Lower maps in Figure 7 show the pattern of transmembrane voltage at the end of the shock and a 5-ms isochrone map of postshock activation. These maps further support the earlier conclusions regarding the propagating nature of the postshock response. The arrows in these maps show the location and direction of the recording sites illustrated in the top panel.

These data are consistent with the idea that excitability may be recovered in refractory tissue if sufficiently negative polarization is produced. As a result, it can be subsequently reexcited if sufficient driving force is provided. What are the possible sources of this driving force, and how it is transmitted?

Relation Between the Postshock Propagation and VE Polarization Amplitude

We previously demonstrated that the VE effect may result in the genesis of new wavefronts of activation.[1] The conduction velocity of a new wavefront depends on both the degree of excitability in the negatively polarized regions and the driving force provided by the positively polarized regions. To investigate this dependence, we analyzed activation maps and maps of transmembrane voltage at the end of shocks of different intensity.

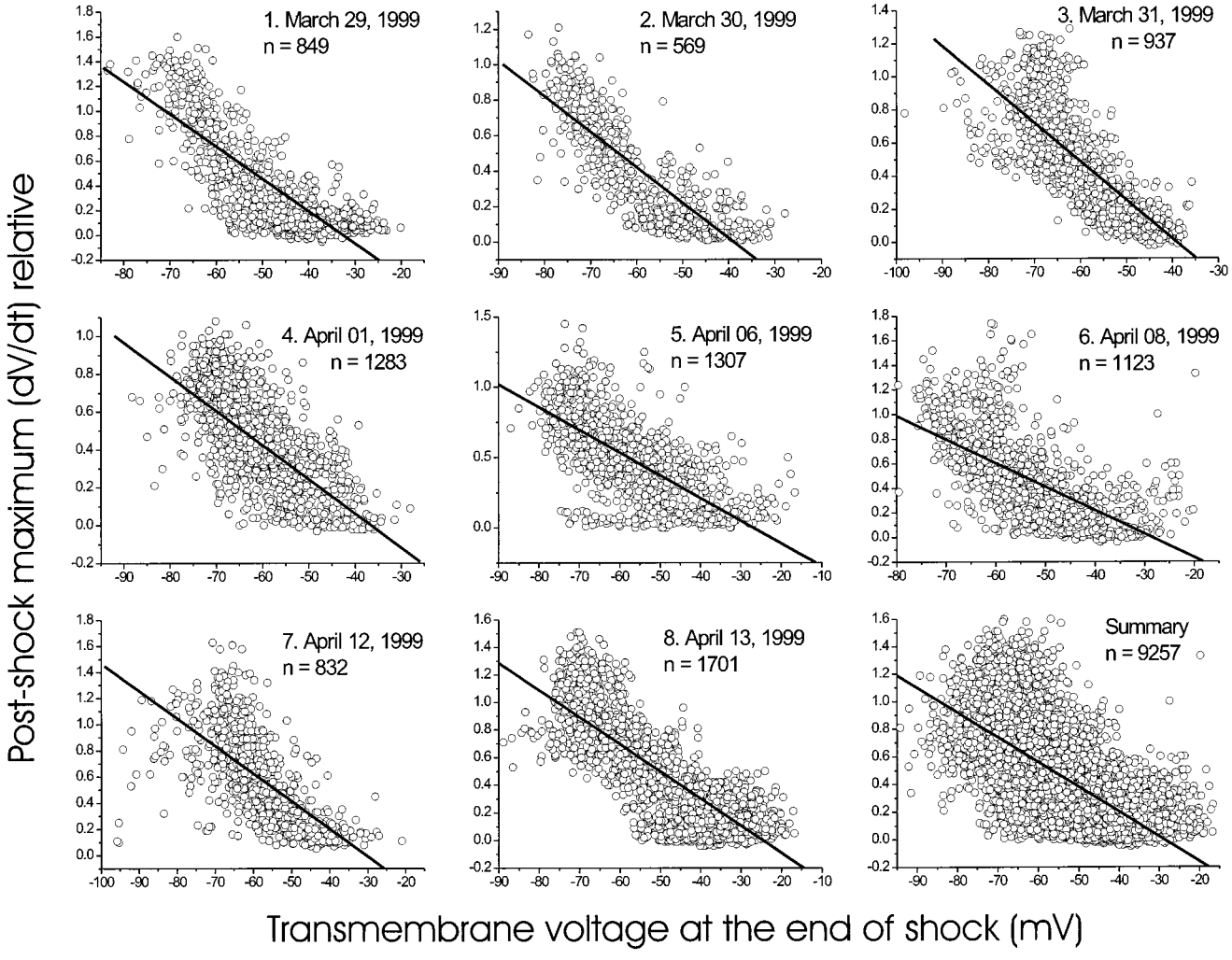

Figure 6. Correlation between rate of rise of postshock response and transmembrane voltage at end of shock. Data from 8 experiments are shown in panels 1 through 8. A summary from these 8 hearts and heart shown in Figure 5 is shown in last panel. Numbers in each panel show number of recordings that were analyzed. Lines represent results of linear regression analysis (see text for details).

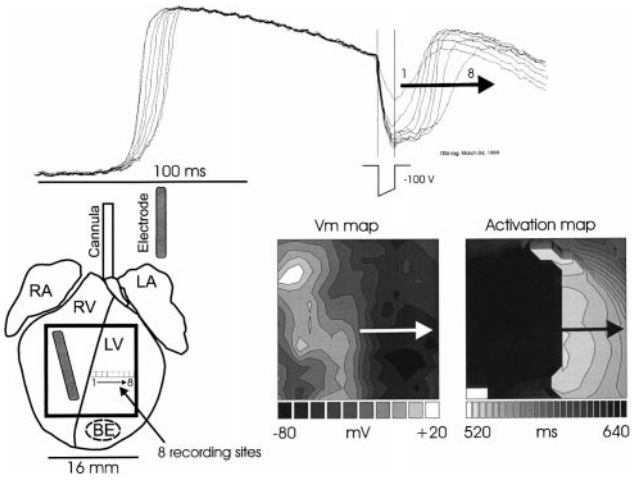

Figure 7. Genesis and conduction of VE-induced wavefront of excitation. Top, 8 representative traces recorded at anterior epicardium during application of a monophasic shock (−100 V, 8 ms). Shock produced negative polarization in all 8 sites. Location of recording sites are shown (bottom left). Bottom middle, Map of transmembrane polarization at end of shock. Bottom right, Map of activation (5-ms isochrone lines) after shock withdrawal at 520 ms. This shock resulted in arrhythmia. Direction and location of arrows in all panels correspond to direction of conduction and location of recording sites. RA indicates right atrium; LA, left atrium; and BE, bipolar electrode.

Figures 8 and 9 illustrate a typical finding. Figure 8A shows that a −80-V shock resulted in VEP with V_m ranging from −4 to −68 mV in positively and negatively polarized regions, respectively. Deexcitation to a transmembrane voltage of ≥−60 mV occurred in the most negatively polarized region at the bottom right of the field of view (dark-blue area). As illustrated in the activation map of Figure 8A, this region was subsequently slowly excited. Incomplete deexcitation (−40 to −60 mV) in the upper right (light blue) precluded the genesis of a wavefront of reexcitation. This region was also subsequently excited, pending its recovery. The wavefront then turned around and produced a reentrant circuit, which resulted in an arrhythmia.

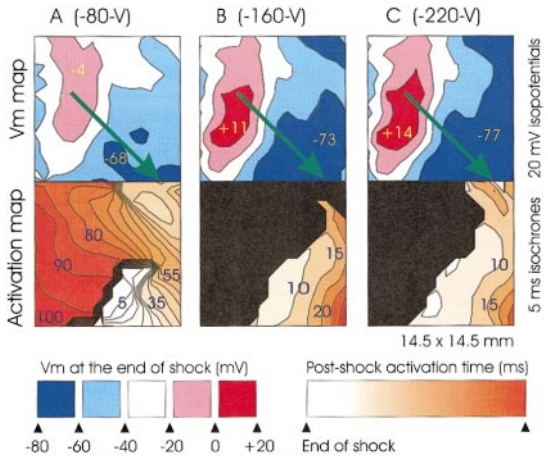

Figure 8. VE polarization and postshock excitation: modulation of conduction velocity and VEP amplitude by shock intensity. Top, Transmembrane voltage at end of shocks. Yellow numbers indicate range of transmembrane voltage reached by VEP. Green arrows show location of recording sites illustrated in Figure 9. Bottom, 5-ms isochrone maps of postshock activation. Numbers indicate time of selected isochronal lines. Areas shown in black were activated by wavefronts, which arrived with significant delay and apparently did not have a causal relationship with postshock excitation. Data were recorded from 14.5×14.5 mm of anterior epicardium. Electrode was located in RV at area of positive polarization. A, B, and C correspond to shock intensities of −80, −160, and −220 V, respectively.

Increasing the shock intensity to −160 V resulted in an increase in both the amplitude and the area of positive and negative polarization. Complete deexcitation (dark-blue area) was now achieved in a significant area occupying the bottom right of the field of view. Thus, a wavefront of reexcitation was produced in a larger area and promptly propagated across the entire deexcited region, reaching the right edge of the field of view only 20 ms after shock withdrawal. Such prompt excitation did not provide sufficient time for recovery of the incompletely deexcited regions; therefore, no reentry was induced by this wavefront. Interestingly, the small area of complete deexcitation in the upper right of Figure 8B (small dark-blue region) was not activated. This was presumably due to the lack of adequate electrotonic interaction between this region and the positively polarized region, which is necessary for wavefront generation. Thus, deexcitation is a required, but not a sufficient, condition for postshock reexcitation. A certain gradient between the positively and negatively polarized regions is also required for the genesis of a postshock wavefront.

Further increase in shock intensity to −220 V (Figure 8C) resulted in complete deexcitation in nearly the entire negatively polarized region (dark-blue area). Such strong deexcitation provided conditions for the genesis of a new wavefront along the entire border between the areas of positive and negative polarization. As in the previous case, no reentry could be produced.

Thus, the conduction velocity of postshock excitation depended on the transmembrane voltage at the end of shock (ie, degree of shock-induced deexcitation).

Figure 9 illustrates the genesis of a VE-induced wavefront with optical recordings taken along the gradient between the positive and negative polarizations. Recording sites are shown with the thick green arrows in V_m maps of Figure 8. Figure 9A shows that −60 mV was barely reached at the end of shock in the area of negative polarization. Nevertheless, due to the strong electrotonic driving force provided from the positively polarized region, a slowly rising and slowly propagating wavefront was generated. Two distal recording sites shown near the arrowhead could not be reached through electrotonus from the positively polarized region due to the great distance. Therefore, they were presumably activated by an active, slowly propagated response. Due to the slow propagation, these sites had more time to repolarize, reaching well below −60 mV. Better recovery resulted in larger amplitudes of the postshock responses and dV/dt_{max}.

Figure 9B illustrates that an increase of shock intensity to −160 V resulted in deexcitation with transmembrane voltages reaching well below −60 mV at the end of shock in all distal sites. In addition, stronger positive polarization provided a stronger driving force, as can be estimated from the magnitude of the transmembrane voltage gradient at the end of shock between positively and negatively polarized sites.

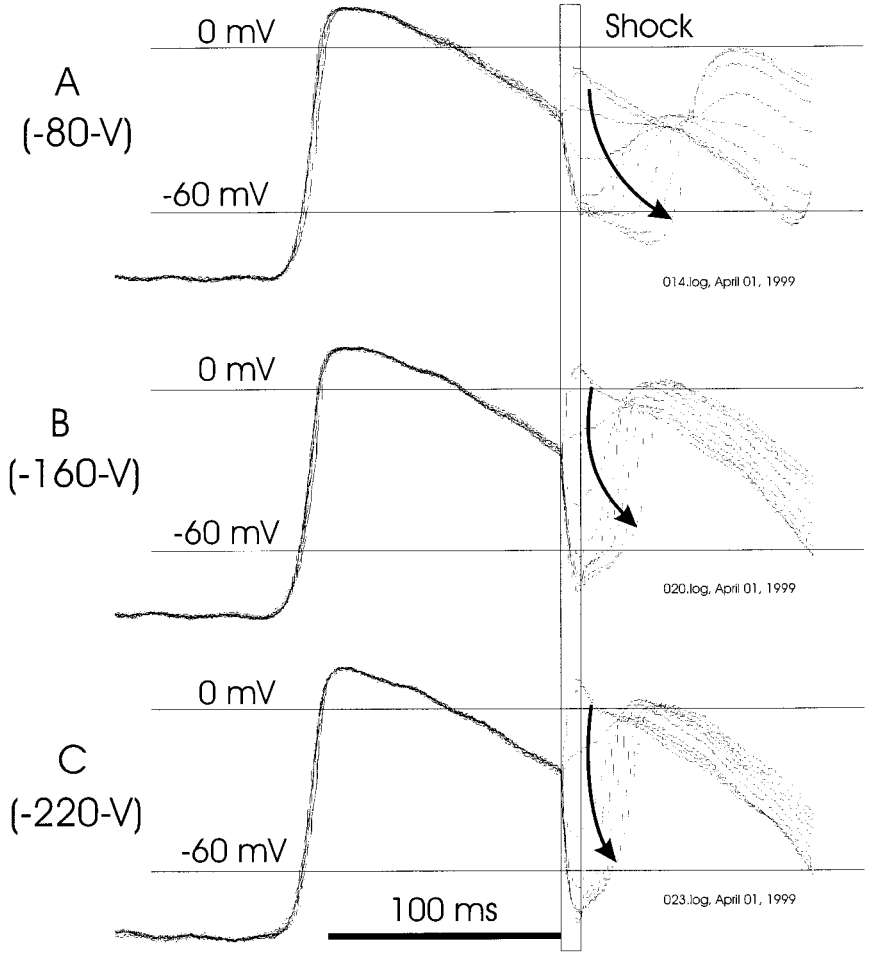

Figure 9. Optical recording during VE-induced wavefront generation and propagation. A through C, 10 representative traces recorded from sites shown with green arrows in top maps of Figure 8. Direction of black arrows in this figure corresponds to direction of green arrows in Figure 8. (See text for details.)

As a result, a vigorous wavefront of reexcitation with nearly normal AP amplitude was generated and rapidly propagated in these sites. A further increase of shock intensity to −220 V (Figure 9C) resulted in stronger negative polarization, a stronger gradient between the 2 opposite polarizations, and faster conduction of the postshock wave of reexcitation.

Correlation Between Negative Polarization and Postshock Activation

Figure 10 summarizes an analysis of the reproducibility of these findings, in which we analyzed the relationship between shock intensity and the rate of rise of postshock activations and transmembrane voltage at the end of shock. As described in Materials and Methods, a fully automated, exhaustively tested computer algorithm was developed to analyze tens of thousands of optical records. Figure 10 shows transmembrane voltage at the end of shocks (last 528 μs) and the rate of rise of postshock excitation as a function of shock intensity. With the criteria described in Materials and Methods, the computer algorithm selected an average of 101.9±29.0 of 256 recording sites per shock, represented as a single data point. The data shown in 9 panels varied with respect to sample size, due to the differences in polarization pattern. The average numbers of recording sites per data point in experiments 1 to 9 were 93.7±6.1, 77.2±16.7, 63.2±7.7, 78.8±22.5, 116.6±10.3, 109.3±21.8, 122.4±15.3, 119.1±11.5, and 141.8±21.4, respectively. Data from a total of 9257 of 23 296 analyzed recordings met the criteria described in Materials and Methods and were included in this figure. The data clearly show progressively more negative V_m values and stronger dV/dt_{max} values with increasing shock intensity.

Discussion

Fibrillation and defibrillation are profoundly complex and poorly understood processes. No known experimental technique can be used to fully assess the electrical activity during these processes with adequate resolution in 3 dimensions. The recent application of voltage-sensitive dyes[17] and imaging techniques[18] to defibrillation research has made it possible to measure electrical activity free of electric field artifacts[3,13,19] with high spatiotemporal resolution.

VE Effect

Using this technology, we demonstrated both that the VE effect is present and that it is likely to play an important role during defibrillation.[1] This was previously theoretically predicted for point stimulation[4] and experimentally demonstrated during epicardial pacing.[20]

The VE effect can occur at macroscopic and microscopic scales due to intramyocardial and extramyocardial heterogeneities and discontinuities. Sepulveda et al[4] predicted that in a two-dimensional bidomain model, areas of opposite polar-

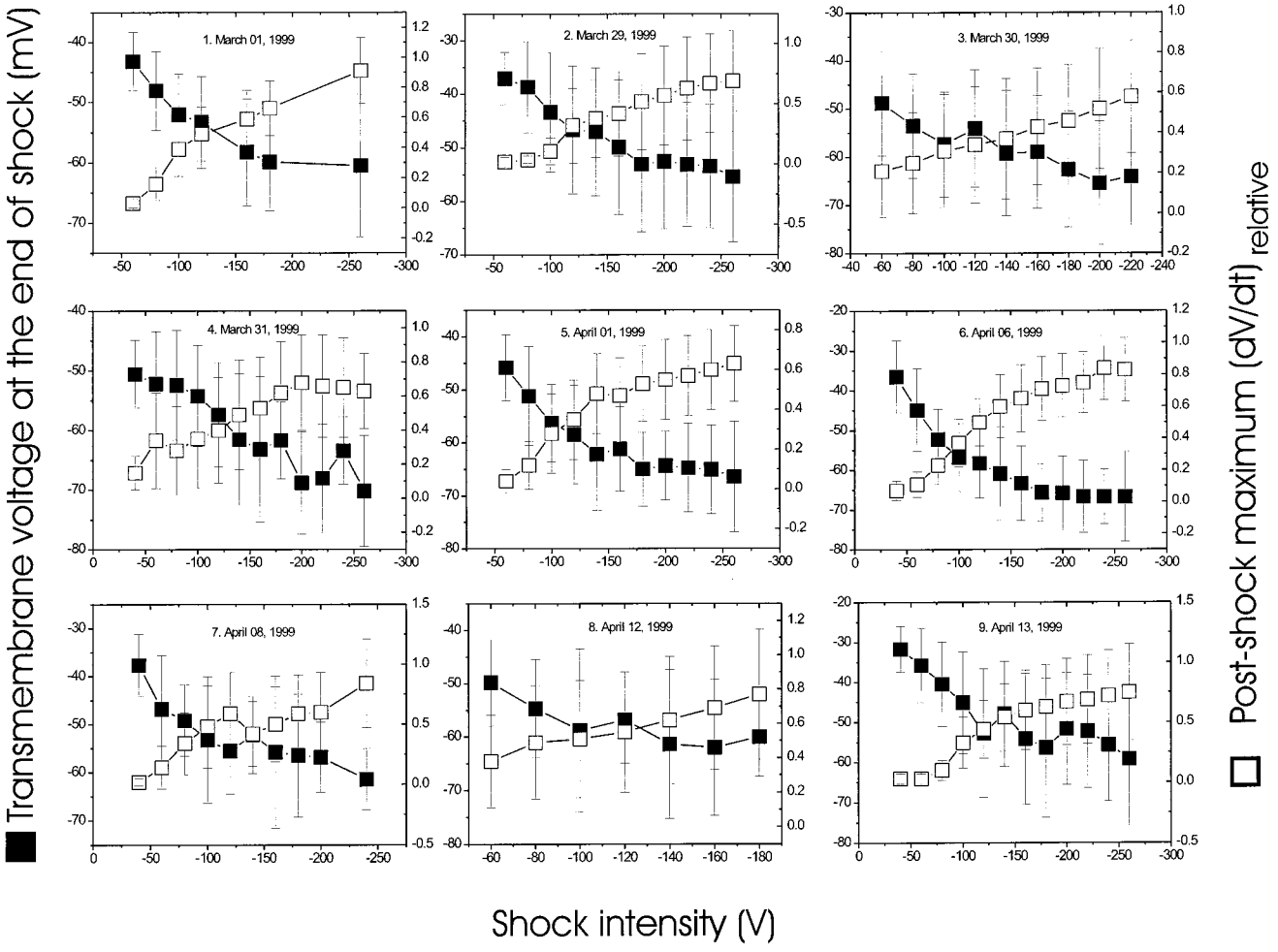

Figure 10. Summary of 9 experiments correlating shock strength (horizontal axis), transmembrane voltage at end of shocks (left vertical axis and data shown with closed boxes), and rate of rise of postshock excitation (right vertical axis and data shown with opened boxes). Rate of rise of postshock excitation in each site was calibrated relative to rate of rise recorded during normal AP upstroke in same site (see Materials and Methods). Each pair of data points (n=91) was calculated from 101.9±29.0 recordings in negatively polarized areas, which were activated between 5 and 30 ms after shock withdrawal.

izations would be induced by epicardial stimuli due to the unequal anisotropic properties of intracellular and extracellular spaces in the myocardium. Roth[21] also predicted that this effect might produce transient wavebreaks, which, however, could not result in sustained reentry. These VEPs were experimentally observed during epicardial pacing by several groups.[20,22,23] A similar, but much stronger, effect was found during defibrillation shocks.[13] Fast et al[24] demonstrated that positive and negative polarizations might be produced by electric shocks at opposite sides of microscopic tissue clefts. These VEs were induced on tissue discontinuities and may produce propagated responses.[24] White et al[25] observed similar effects on a macroscopic scale. Trayanova[26] predicted, using a bidomain model, that areas of opposite polarizations can occur at any tissue/bath interface.

Despite apparent differences in the exact mechanism of VE effect, it appears to be produced primarily by passive structural heterogeneities/discontinuities. These modulate and redistribute extracellularly applied fields, producing an inward or outward activating current in different parts of the myocardium. This current produces positive or negative polarizations, respectively. The general nature of the mechanism was best expressed by Sobie et al.[27] One might argue that during extracellularly applied fields, no net current flow across the membrane would occur. Thus, the presence of areas of opposite polarization next to each other is a consequence of the redistribution of charges between neighboring regions of the syncytium, next to the discontinuity/heterogeneity. Therefore, a single myocyte, being a part of the syncytium, may undergo transmembrane polarization due to macroscopic charge redistribution within intracellular or extracellular domains without actual transmembrane current injection.

Relation Between Break Excitation and Reexcitation Wavefront Mechanisms

Break excitation has been proposed to explain the mechanisms of pacing based on VE effect.[20] According to this mechanism, negatively polarized areas will be simultaneously activated after the withdrawal of a long stimulus by an electrotonically transmitted driving force from neighboring positively polarized area. During defibrillation, this may not be exactly the same because of scale differences. Indeed,

negatively polarized areas, although fully excitable, can extend to large distances, comparable with the size of the entire ventricle.[13] Clearly, electrotonic transmission cannot reach such remote areas. Break excitation can only initiate new wavefronts at the boundary between positively and negatively polarized areas, which then propagate across the negatively polarized region, as demonstrated in this study.

Alternative theory of break excitation suggested that the postshock depolarization may result from hyperpolarization-activated I_F current.[28] Unfortunately, our data do not provide direct verification of this hypothesis, because the degree of negative polarization observed in our study was insufficient to open I_F current. Additional studies are required to evaluate the contribution of the mechanism of break excitation of Ranjan et al[28] to defibrillation.

VE-Induced Reexcitation: Mechanism of Defibrillation

The VE effect has dual roles in defibrillation. Due to this effect, a monophasic defibrillation shock of any polarity can erase preexisting fibrillatory activity by rapidly resetting the phase and inducing positive and negative polarization in neighboring areas. However, at the same time, this effect may create a new arrhythmia via induction of VE-induced phase singularities.[1]

This report shows that conduction velocity and AP rate of rise of a postshock reexcitation wavefront depends on the transmembrane voltage in negatively polarized areas (see Figures 5 through 10). Conduction can be very slow and discontinuous with unidirectional blocks when deexcitation is insufficient. Perhaps such slow, discontinuous conduction is supported when polarization resulted in recovery from inactivation of calcium but not sodium channels (see Figure 8A). In this case, phase singularities and arrhythmias are induced, leading to defibrillation failure.[1]

As we recently demonstrated, optimal biphasic defibrillation shocks can cancel the VEs and the phase singularity resulting from it.[1] Effective second phases of optimal defibrillation waveforms cancel the VE effect produced by the first phase. This may be the best scenario for successful defibrillation, because no dispersion of repolarization or new propagated wavefronts will be induced by the shock. This mechanism is likely to underlie type A defibrillation with no postshock responses.

Alternatively, successful defibrillation may result from shocks producing strong VE polarizations. In this case, negatively polarized areas will be rapidly reexcited by break excitation–induced propagated responses. Reexcitation can be completed within milliseconds after the shock (Figure 8C). Although wavebreaks may be induced, they do not result in sustained arrhythmias, because of the rapid conduction velocity and the long wavelength of the shock-induced response. This mechanism may underlie type B defibrillation, characterized by the occurrence of a few extra beats induced by wavebreaks.

Implications to Lower and Upper Limits of Vulnerability

Chen et al[29] was first to point out that the proarrhythmic and antiarrhythmic effects of strong electric shocks are in a causal relationship, proposing the upper limit of vulnerability theory. Our data indicate that progressive increases in shock intensity will result in passing 2 distinct thresholds, with the separation of fundamentally different proarrhythmic responses produced by VEs. First, the weakest shocks will produce prolongation and shortening of APs in areas of positive and negative polarization, respectively. This will produce a dispersion of repolarization but will not result in shock-induced wavefronts and therefore cannot be proarrhythmic (Figure 2). Further increases in shock intensity will result in recovery from inactivation in some areas and will result in the creation of both dispersion of repolarization and reexcitation wavefronts (Figures 1 and 3). VE-induced phase singularity and slow conduction will result in the genesis of arrhythmias. The threshold in shock intensity between these 2 types of responses may correspond to the lower limit of vulnerability. Further gradual increases in shock intensity will result in a gradually stronger negative polarization and more rapid reexcitation. At some shock voltage, the reexcitation wavelength will be too long to sustain the reentrant circuit (Figure 8B and 8C); therefore, no sustained arrhythmia will be induced, and the upper limit of vulnerability will be reached.

Study Limitations

We recently demonstrated that the VE phenomenon is essentially 3-dimensional.[30] Therefore, the 2-dimensional mapping technique used in this study provides somewhat limited insights into the mechanism. For instance, the driving force may come from deeper layers of the myocardium, which may introduce a distortion in the spatial correlation between postshock transmembrane polarizations and resulting propagation. Nevertheless, our data strongly indicate that the observed phenomenon of shock-induced reexcitation by propagated wavefronts can be easily extended to the 3-dimensional situation. Unfortunately, no experimental technique is available at present to assess the 3-dimensional map of electrical activity. Computer simulations may provide the missing link between passive bidomain predictions of VE effects and the resulting 3-dimensional pattern of electrical activity.

The possible impact of BDM has been previously addressed.[13] BDM has limited effects on the APD of rabbit atrioventricular nodal cells[31] and ventricular cells.[32] However, the effects of BDM on shock-induced responses remain to be investigated.

Acknowledgments

This work was supported by NIH grants R01-HL59464 and R01-HL58808 and American Heart Association, Northeast Ohio Affiliate, Grant-in-Aid 9806201. We thank Dr D. W. Wallick for careful review of the manuscript.

References

1. Efimov IR, Cheng Y, Van Wagoner DR, Mazgalev T, Tchou PJ. Virtual electrode-induced phase singularity: a basic mechanism of failure to defibrillate. *Circ Res*. 1998;82:918–925.
2. Witkowski FX, Penkoske PA. Refractoriness prolongation by defibrillation shocks. *Circulation*. 1990;82:1064–1066.

3. Dillon SM. Synchronized repolarization after defibrillation shocks: a possible component of the defibrillation process demonstrated by optical recordings in rabbit heart. *Circulation*. 1992;85:1865–1878.
4. Sepulveda NG, Roth BJ, Wikswo JP Jr. Current injection into a two-dimensional anisotropic bidomain. *Biophys J*. 1989;55:987–999.
5. Walcott GP, Knisley SB, Zhou X, Newton JC, Ideker RE. On the mechanism of ventricular defibrillation. *Pacing Clin Electrophysiol*. 1997;20:422–431.
6. Chen PS, Wolf PD, Ideker RE. Mechanism of cardiac defibrillation: a different point of view. *Circulation*. 1991;84:913–919.
7. Frazier DW, Wolf PD, Wharton JM, Tang AS, Smith WM, Ideker RE. Stimulus-induced critical point: mechanism for electrical initiation of reentry in normal canine myocardium. *J Clin Invest*. 1989;83:1039–1052.
8. Kwaku KF, Dillon SM. Shock-induced depolarization of refractory myocardium prevents wave-front propagation in defibrillation. *Circ Res*. 1996;79:957–973.
9. Weidmann S. Effect of current flow on the membrane potential of cardiac muscle. *J Physiol*. 1951;115:227–236.
10. Chang JJ, Schmidt, RF. Prolonged action potentials and regenerative repolarization responses in Purkinje fibers of mammalian heart. *Arch Physiol*. 1960;272:127–140.
11. Hall AE, Noble D. Transient responses of Purkinje fibers to non-uniform currents. *Nature*. 1963;199:1294–1295.
12. Vassale M. Analysis of cardiac pacemaker potential using a "voltage clamp" technique. *Am J Physiol*. 1966;210:1335–1341.
13. Efimov IR, Cheng YN, Biermann M, Van Wagoner DR, Mazgalev T, Tchou PJ. Transmembrane voltage changes produced by real and virtual electrodes during monophasic defibrillation shock delivered by an implantable electrode. *J Cardiovasc Electrophysiol*. 1997;8:1031–1045.
14. Gray RA, Ayers G, Jalife J. Video imaging of atrial defibrillation in the sheep heart. *Circulation*. 1997;95:1038–1047.
15. Girouard SD, Laurita KR, Rosenbaum, DS. Unique properties of cardiac action potentials recorded with voltage-sensitive dyes. *J Cardiovasc Electrophysiol*. 1996;7:1024–1038.
16. Dillon SM, Mehra R. Prolongation of ventricular refractoriness by defibrillaion shocks may be due to additional depolarization of the action potential. *J Cardiovasc Electrophysiol*. 1992;3:442–456.
17. Davila HV, Salzberg BM, Cohen LB, Waggoner AS. A large change in axon fluorescence that provides a promising method for measuring membrane potential. *Nat New Biol*. 1973;241:159–160.
18. Grinvald A, Cohen LB, Lesher S, Boyle MB. Simultaneous optical monitoring of activity of many neurons in invertebrate ganglia using a 124-element photodiode array. *J Neurophysiol*. 1981;45:829–840.
19. Zhou X, Ideker RE, Blitchington TF, Smith WM, Knisley SB. Optical transmembrane potential measurements during defibrillation-strength shocks in perfused rabbit hearts. *Circ Res*. 1995;77:593–602.
20. Wikswo JP, Lin S-F, Abbas RA. Virtual electrodes in cardiac tissue: a common mechanism for anodal and cathodal stimulation. *Biophys J*. 1995;69:2195–2210.
21. Roth BJ. A mathematical model of make and break electrical stimulation of cardiac tissue by a unipolar anode or cathode. *IEEE Trans Biomed Eng*. 1995;42:1174–1184.
22. Knisley SB, Hill BC, Ideker RE. Virtual electrode effects in myocardial fibers. *Biophys J*. 1994;66:719–728.
23. Neunlist M, Tung L. Spatial distribution of cardiac transmembrane potentials around an extracellular electrode: dependence on fiber orientation. *Biophys J*. 1995;68:2310–2322.
24. Fast VG, Rohr S, Gillis AM, Kleber AG. Activation of cardiac tissue by extracellular electrical shocks: formation of "secondary sources" at intercellular clefts in monolayers of cultured myocytes. *Circ Res*. 1998;82:375–385.
25. White JB, Walcott GP, Pollard AE, Ideker RE. Myocardial discontinuities: a substrate for producing virtual electrodes that directly excite the myocardium by shocks. *Circ*. 1998;97:1738–1745.
26. Trayanova NA. Effects of the tissue-bath interface on the induced transmembrane potential: a modeling study in cardiac stimulation. *Ann Biomed Eng*. 1997;25:783–792.
27. Sobie EA, Susil RC, Tung L. A generalized activating function for predicting virtual electrodes in cardiac tissue. *Biophys J*. 1997;73:1410–1423.
28. Ranjan R, Chiamvimonvat N, Thakor NV, Tomaselli GF, Marban E. Mechanism of anode break stimulation in the heart. *Biophys J*. 1998;74:1850–1863.
29. Chen PS, Shibata N, Dixon EG, Martin RO, Ideker RE. Comparison of the defibrillation threshold and the upper limit of ventricular vulnerability. *Circulation*. 1986;73:1022–1028.
30. Entcheva E, Eason J, Efimov IR, Cheng Y, Malkin RA, Claydon F. Virtual electrode effects in transvenous defibrillation: modulation by structure and interface: evidence from bidomain simulations and optical mapping. *J Cardiovasc Electrophysiol*. 1998;9:949–961.
31. Cheng Y, Mowrey KA, Efimov IR, Van Wagoner DR, Tchou PJ, Mazgalev TN. Effects of 2,3-butanedione monoxime on the atrial-atrioventricular nodal conduction in isolated rabbit heart. *J Cardiovasc Electrophysiol*. 1997;8:790–802.
32. Tovar O, Amanna A, Milne K, Krauthamer V, Jones J. Effects of diacetyl monoxime on cardiac action potential duration and fibrillation cycle length. *Pacing Clin Electrophysiol*. 1994;17(II):824. Abstract.